Efficient Direct Solution of EFIE for Electrically Large Scattering Problems using $\mathcal{H}$-LDLT and PE Basis Function

Ting Wan, Rushan Chen, Xiaoqing Hu, Yilin Chen, and Yijun Sheng

Department of Communication Engineering
Nanjing University of Science and Technology, Nanjing, 210094, China
billwanting@163.com

Abstract ─ Method of moments (MoM) solution of the electric field integral equations (EFIE) encounters the large memory requirements and the slow convergence rate of the iterative solver. A direct method based on hierarchical ($\mathcal{H}$-) matrix algorithm and phase extracted (PE) basis function is proposed to overcome these obstacles. A recompressed adaptive cross approximation (ACA) technique is employed to generate a data-sparse representation of the dense EFIE system matrix, i.e., so-called $\mathcal{H}$-matrix. $\mathcal{H}$-matrix formatted LDLT-decomposition ($\mathcal{H}$-LDLT) can be implemented in nearly optimal complexity, which provides an efficient way for the direct solution of EFIE. PE basis function, containing the propagating wave phase factor and defined on large patches, is introduced to further reduce the computational costs. Numerical results demonstrate the accuracy and efficiency of the proposed method for electrically large scattering problems.

Index Terms ─ Direct solution, electrically large scattering, hierarchical LDLT-decomposition ($\mathcal{H}$-LDLT), phase extracted (PE) basis function, recompressed adaptive cross approximation (ACA).

I. INTRODUCTION

The electric-field integral equation (EFIE) is widely used to analyze electromagnetic scattering since it can handle fairly general geometries [1]. The method of moments (MoM) is a powerful technique for the solution of EFIE. Numerical discretization of the EFIE by MoM [2] yields a dense complex linear system, which is a serious handicap especially for electrically large scattering problems. Two distinct approaches have recently emerged to address this issue. The first concerns efficient methods for the solution of the large dense linear system. The second directly pursue a reduction of the number of unknowns required to obtain an accurate result. In respect of the first point, methods for the numerical solution of the linear system can usually be classified into two categories, i.e., direct methods and iterative methods. It is basically impractical to use direct methods due to the $O(N^2)$ memory requirement and $O(N^3)$ computational complexity, where N refers to the number of unknowns. This can be circumvented by iterative methods, in which the required matrix-vector product operation can be accelerated by multilevel fast multipole method (MLFMM) [3-6]. However, a linear system resulting from EFIE is usually ill-conditioned, particularly for electrically large problems. Effective preconditioners can be used to accelerate the convergence rate of iterations, but they are usually problem-dependent [7,8]. Moreover, for electrically large problems, the memory is still burdened due to the filling of near-interaction blocks. As the second approach mentioned above, other interesting contributions attempt to reduce the complexity by considering more elaborate bases to approximate the unknown field, such as, the physical optics (PO) method, geometrical optics (GO) method, and characteristic basis function (CBF) method [9-12]. Besides, a kind of basis functions with phase information, named phase extracted (PE) basis functions, has recently been presented [13-15]. Since the induced currents

Submitted On: July 7, 2011
Accepted On: August 12, 2011

on the smooth PEC surface have the propagating wave phase dependency, the PE bases can be defined on very large patches.

Combining the two approaches mentioned above, in this paper, an efficient direct method based on hierarchical LDLT-decomposition ($\mathcal{H}$-LDLT) algorithm and PE basis function is presented to improve the MoM solution of EFIE. $\mathcal{H}$-matrix algorithm are based on the data-sparse representation, which is an inexpensive but sufficiently accurate way to approximate a fully populated matrix [16-18]. The key idea is to approximate a full matrix by a product of two low-rank matrices [16,19]. In this paper, the adaptive cross approximation (ACA) algorithm is used to generate the low-rank approximations [20-23]. A major advantage of ACA is that it deals only with the matrix entries and is, therefore, kernel-independent in contrast to other compression methods like fast multipole [3], panel clustering [24], or the $\mathcal{H}^2$-matrix approximation [25] that are based on expansions or interpolations of the kernel-function. Hence, a practical advantage of ACA is that it can be built on top of existing computer codes without changes. A blockwise recompression scheme is applied following ACA to decrease the memory usage. The essential operations of $\mathcal{H}$-matrices, such as matrix-vector and matrix-matrix multiplication, addition, and LU decomposition, can be performed through $\mathcal{H}$-matrix arithmetic in $O(k^a N \log^b N)$ complexity with blockwise rank k and appropriate parameters a, b [26]. The PE basis function is introduced to reduce the number of unknowns, which creates more favourable conditions for the implement of $\mathcal{H}$-LDLT. Expressing the propagating wave phase dependency, the PE bases break the well-known convention of '10 degrees of freedom per wavelength' and can be defined on the patches with much larger electrical size. Hence, the use of PE basis functions leads to a dramatically computational saving. Numerical examples will show that the proposed method can significantly reduce the memory requirement and computational complexity compared with the traditional direct method and is robust for electrically large scattering problems.

The remainder of this paper is organized as follows: Section II describes the theory and implementation of PE basis functions, the recompressed ACA technique, and the $\mathcal{H}$-LDLT algorithm in detail. Numerical experiments with several electrically large scattering problems are presented to demonstrate the efficiency of the proposed method in Section III. Section IV gives some conclusions.

II. THEORY

A. MoM solution of EFIE with phase extracted basis functions

Consider an arbitrarily-shaped 3D conducting object illuminated by an incident field $\mathbf{E}^i(\mathbf{r})$. The EFIE is given by

$$\hat{n} \times \iint_S \bar{\boldsymbol{G}}(\mathbf{r},\mathbf{r}') \mathbf{J}(\mathbf{r}') d\mathbf{r}' = \frac{1}{jk_0\eta_0} \hat{n} \times \mathbf{E}^i(\mathbf{r}) \text{ on } S, \quad (1)$$

where S denotes the conducting surface of the object, $\hat{n}$ is an outwardly directed normal, $\bar{\boldsymbol{G}}(\mathbf{r},\mathbf{r}')$ is the well-known free-space Green's function, and J(r) denotes the unknown surface current.

For the scattering excited by a plane wave in the homogeneous background medium, the tangential component of the incident magnetic field contains a propagating wave phase dependency, which can be expressed as

$$\mathbf{H}_t^{inc} \sim e^{-j\mathbf{k}^i \cdot \mathbf{r}}, \quad (2)$$

where $\mathbf{k}^i$ is the propagation vector of the incident wave in the background medium. (2) indicates $\nabla \cdot \mathbf{H}_t^{inc} \sim e^{-j\mathbf{k}^i \cdot \mathbf{r}}$. Expressing the tangential component of the total magnetic field as the summation of the tangential component of incident and the scattering magnetic field, and considering the boundary condition that the normal component of magnetic field vanishes on the PEC surface, we have

$$\nabla \cdot \mathbf{H}_t = \nabla \cdot \mathbf{H}_t^{inc} + \nabla \cdot \mathbf{H}_t^{sca} = 0. \quad (3)$$

Hence, the total magnetic field also has the phase dependency. According to the surface equivalence theorem, the induced current, and the total magnetic field satisfy $\mathbf{J} = \hat{\mathbf{n}} \times \mathbf{H}$, thus, it can be concluded that the induced current on the PEC surface has the propagating wave phase property:

$$\mathbf{J}_t^{inc} \sim e^{-j\mathbf{k}^i \cdot \mathbf{r}}. \quad (4)$$

Based on this, a basis function with the propagating wave phase factor is introduced, called phase extracted (PE) basis functions. PE

basis functions can be expressed as the multiplication of an amplitude term and a phase term. The amplitude term here is chosen as a triangular curvilinear Rao-Wilton-Glisson (CRWG) function in conventional MoM formulation due to its accuracy in representing arbitrary curvilinear surfaces, and the phase term is an exponential function, as follows

$$\mathbf{J}_n(\mathbf{r}) = \mathbf{j}_n(\mathbf{r}) e^{-j\mathbf{k}^i \cdot \mathbf{r}}, \tag{5}$$

where $\mathbf{j}_n(\mathbf{r})$ denotes the CRWG basis functions. Thus, the induced current $\mathbf{J}(\mathbf{r})$ can be expanded with the PE basis functions $\mathbf{J}_n(\mathbf{r})$:

$$\mathbf{J}(\mathbf{r}) = \sum_{n=1}^{N} a_n \mathbf{j}_n(\mathbf{r}) e^{-j\mathbf{k}^i \cdot \mathbf{r}}. \tag{6}$$

After the phase extraction, the residual part of the basis needs to express the amplitude distribution only. For convex objects with smooth surfaces, the amplitude term of the induced current varies much slower compared with the oscillatory phase term. As a result, they can be defined on much larger patches than the traditional basis functions which do not involve any phase information. Hence, a set of very coarse mesh grid can be used to discretize the objects and the number of basis functions can be reduced dramatically. Away from the smooth region, where the PE basis function becomes invalid, the ordinary discretization density of conventional CRWG basis functions is needed. After Galerkin's testing, the resulting linear system from EFIE formulation can be symbolically rewritten as

$$Ax=b, \tag{7}$$

where A denotes the system matrix with the size being the number of PE basis functions.

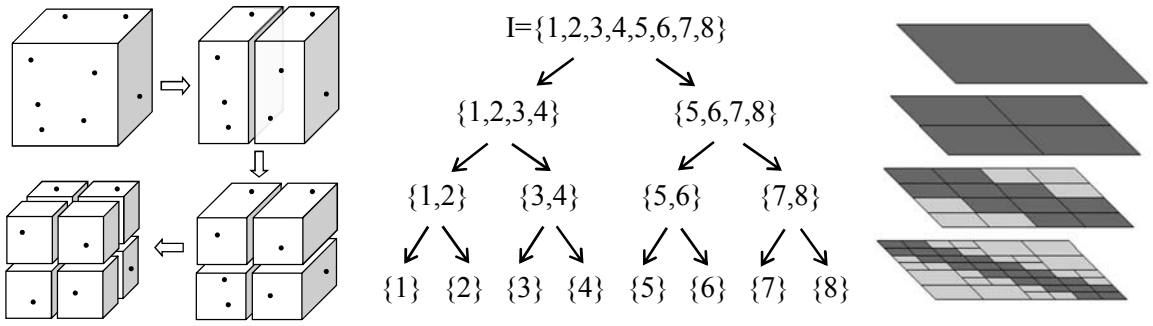

Fig. 1. (a) Subdivision of a finite set using bounding box. " • " denotes the midpoint of each edge. (b) Cluster tree T_I. (c) Block cluster tree $T_{I\times I}$. Admissible leaves are *light grey*.

B. Construct an $\mathcal{H}$-matrix by hierarchical partitioning

The process of generating an $\mathcal{H}$-matrix representation of the EFIE system matrix A is performed by two main procedures. They are the hierarchical partitioning of the matrix into blocks and the blockwise restriction to low-rank matrices. The hierarchical partitioning is on the basis of a *cluster tree*, i.e., a tree T_I satisfies the following:

- $\mathrm{root}(T_I) = I$,
- if $t \in T_I$ with $\mathrm{sons}(t) \neq \varnothing$, then $t = \bigcup\{t' : t' \in \mathrm{sons}(t)\}$,
- if $t \in T_I$ with $\mathrm{sons}(t) = \varnothing$, then $\#t \le n_{\min}$.

where $I = \{1,2,\ldots\ldots N\}$ is a finite index set of all the PE basis functions, $\#t$ denotes the number of elements in the cluster t and $n_{\min}$ is a predetermined threshold parameter to control the depth of the cluster tree. A simple method for building a cluster tree is bisection based on geometry-based subdivisions of the index sets using bounding boxes. The key idea of this method is to split an index set in the coordinate direction of maximal extent. Figure 1 (a) depicts a simplified subdivision with I including only eight elements, and the resulting binary cluster tree T_I is shown in Fig. 1 (b).

Based on the cluster tree T_I, the index set $I \times I$ corresponding to the system matrix $\mathbf{A} \in \mathbb{C}^{I \times I}$ is split into a partition

$$P = \{t \times s : t, s \in T_I\}, \tag{8}$$

which generates the *block cluster tree* $T_{I \times I}$. To approximate a matrix by a block-wise low-rank approximation, the sub-blocks have to fulfill a so-called admissibility condition as follows

$$\max\{diam(B_t), diam(B_s)\} \le \eta dist(B_t, B_s), \tag{9}$$

where B_t and B_s denotes the minimal bounding box for the support of cluster *t* and *s*, *diam* and *dist* denote the Euclidean diameter and distance of cluster *t* and *s* respectively, and $\eta \in \mathbb{R}^+$ controls the trade-off between the number of admissible blocks. Based on this, the partitioning *P* can be split into admissible ("far-field") and inadmissible ("near-field") blocks described as:

$$P = P^{near} \bigcup P^{far}, \tag{10}$$

with

$$P^{far} = \{t \times s \in P : \text{(9) holds}\}, \tag{11}$$

where admissible blocks can be approximated by low-rank representation in the following Rk-matrices as follows

$$M|_{m \times n} = AB^H, \quad A \in \mathbb{C}^{m \times k}, B \in \mathbb{C}^{n \times k}, \tag{12}$$

with *A*, *B* in full matrix representation, and *k* is much smaller than *m* and *n*. The corresponding block cluster tree $T_{I \times I}$ based on the cluster tree T_I of Fig. 1 (b) is given in Fig. 1 (c).

Based on the cluster tree and the block cluster tree, the class of $\mathcal{H}$-matrix for an admissible partitioning *P* and the maximum rank *k* can be defined as

$$\mathcal{H}(P,k) := \left\{A \in \mathbb{C}^{I \times I} : \text{rank}(A|_b) \le k \text{ for all } b \in P\right\}. \tag{13}$$

C. Low-rank approximation using recompressed ACA

In the $\mathcal{H}$-matrix representation, near-field blocks are uncompressed and to be computed via PE-based MoM. Due to the rapid decay of the discrete Green's function, the far-field blocks can be compressed to low-rank representations with little loss of accuracy. To find these low-rank approximations, the adaptive cross approximation (ACA) algorithm is adopted. In this algorithm, the normally dense far-field blocks are approximated by using only a few rows and columns, i.e., crosses of these blocks, while other matrix entries are not required to be calculated. Starting from only one cross and adding more and more crosses, one applies this approximation iteratively until the difference between two consecutive cross-approximations are small enough. Then, the low-rank approximations of the far-field blocks are achieved. Since the ACA theory can be found in the original work of Bebendorf [20,21], the details of it will not be presented in this paper. It is worth noting that the low-rank representation obtained by ACA is not yet optimal in terms of storage requirements. These low-rank blocks can be in fact recompressed, using QR decomposition and the truncated singular value decomposition (SVD), which allows a further storage reduction without accuracy penalties. The process of recompressing a low-rank block $M = AB^H$ to $\tilde{M} = \tilde{A}\tilde{B}^H$ can be performed as follows:

1. Compute a QR decomposition $A = Q_A R_A$, $Q_A \in \mathbb{C}^{m \times k}$, $R_A \in \mathbb{C}^{k \times k}$.
2. Compute a QR decomposition $B = Q_B R_B$, $Q_B \in \mathbb{C}^{n \times k}$, $R_B \in \mathbb{C}^{k \times k}$.
3. Compute a singular value decomposition $R_A R_B^H = U \sum V^H$.
4. Extract $\tilde{\sum} = \text{diag}(\sum_{11}, \sum_{22} \cdots, \sum_{k'k'})$ (first largest k' singular values) with k' satisfies $\sum_{k'k'} > \varepsilon_{\text{ACA}} \sum_{11}$ and $\sum_{(k'+1)(k'+1)} \le \varepsilon_{\text{ACA}} \sum_{11}$, where ε_{ACA} is the relative truncation error.
5. Extract $\tilde{U} = [U_1\ U_2 \cdots U_{k'}]$ (first k' columns), $\tilde{V} = [V_1\ V_2 \cdots V_{k'}]$ (first k' columns).
6. Set $\tilde{A} = Q_A \tilde{U} \tilde{\sum}$ and $\tilde{B} = Q_B \tilde{V}$.

Thus, the construction of an $\mathcal{H}$-matrix is accomplished with its admissible blocks generating from the recompressed ACA technique. A typical structure of an $\mathcal{H}$-matrix in practice is presented in Fig. 2.

D. The recursive scheme for $\mathcal{H}$-LDLT

The $\mathcal{H}$-LDLT decomposition can be implemented recursively starting from a 2×2 block-matrix induced by the hierarchical partitioning. Using the exact LDLT decomposition on the finest level and assuming that the $\mathcal{H}$-LDLT decomposition has already been defined on all finer

levels, the unknown blocks L_{ij}, D_{ii}, and U_{ij} can be solved in the following three steps:

$$\mathcal{H}=\begin{bmatrix}\mathcal{H}_{11} & \mathcal{H}_{12}\\ \mathcal{H}_{21} & \mathcal{H}_{22}\end{bmatrix}=\begin{bmatrix}L_{11} & \\ L_{21} & L_{22}\end{bmatrix}\begin{bmatrix}D_{11} & \\ & D_{22}\end{bmatrix}\begin{bmatrix}L_{11}^{\mathrm{T}} & L_{21}^{\mathrm{T}}\\ & L_{22}^{\mathrm{T}}\end{bmatrix}. \quad (14)$$

1. Compute L_{11} and D_{11} from $\mathcal{H}_{11}=L_{11}D_{11}L_{11}^{\mathrm{T}}$ by an $\mathcal{H}$-LDLT decomposition on the next finer level.
2. Compute L_{21} from $\mathcal{H}_{21}=L_{21}D_{11}L_{11}^{\mathrm{T}}$ by an upper triangular solver.
3. Compute L_{22} and D_{22} from $\mathcal{H}_{22}-L_{21}D_{11}L_{21}^{\mathrm{T}}=L_{22}D_{22}L_{22}^{\mathrm{T}}$ by an $\mathcal{H}$-LDLT decomposition on the next finer level.

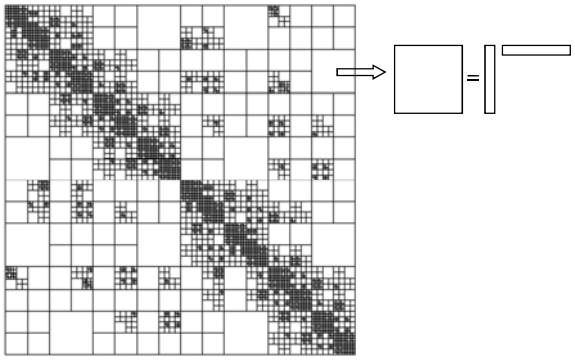

Fig. 2. A typical $\mathcal{H}$-matrix with ACA-based low-rank matrices.

In Step 2 above, an upper triangular solver is needed to solve a upper triangular system, with a given upper triangular matrix $D_{11}L_{11}^{\mathrm{T}}$ and a given right-hand-side matrix $\mathcal{H}_{21}$, simplified as $XU=B$. It can also be solved recursively from

$$\begin{bmatrix}X_{11} & X_{12}\\ X_{21} & X_{22}\end{bmatrix}\begin{bmatrix}U_{11} & U_{12}\\ & U_{22}\end{bmatrix}=\begin{bmatrix}B_{11} & B_{12}\\ B_{21} & B_{22}\end{bmatrix}. \quad (15)$$

in the following four steps:

1. Compute X_{11} from $X_{11}U_{11}=B_{11}$ by an upper triangular solver on the next finer level.
2. Compute X_{21} from $X_{21}U_{11}=B_{21}$ by an upper triangular solver on the next finer level.
3. Compute X_{12} from $X_{12}U_{22}=B_{12}-X_{11}U_{12}$ by an upper triangular solver on the next finer level.
4. Compute X_{22} from $X_{22}U_{22}=B_{22}-X_{21}U_{12}$ by an upper triangular solver on the next finer level.

In all these steps for the $\mathcal{H}$-LDLT decomposition and the upper triangular solver, the exact addition and multiplication are replaced by the faster formatted $\mathcal{H}$-matrix counterparts ($\oplus$ and $\otimes$). Truncation operator $\mathcal{T}_{k\leftarrow k'}^{\mathcal{H}}$ based on truncated versions of the *QR*-decomposition and singular value decomposition (SVD) is used to define the $\mathcal{H}$-matrix addition $A\oplus B=\mathcal{T}_{k\leftarrow 2k}^{\mathcal{H}}(A+B)$ and the $\mathcal{H}$-matrix multiplication $A\otimes B=\mathcal{T}_{k\leftarrow k'}^{\mathcal{H}}(A\times B)$. In this paper, an adaptive truncation scheme with a relative truncation error $\varepsilon_{\mathcal{H}}$ is adopted, similarly defined as $\varepsilon_{\mathrm{ACA}}$. It should be noted that matrix D is the diagonal matrix with little additional storage consumption. $\mathcal{H}$-LDLT can be performed in $O(k^2N\log^2N)$ computational complexity and $O(kN\log N)$ storage requirement with blockwise rank k. After the completion of $\mathcal{H}$-LDLT decomposition, $\mathcal{H}$-matrix formatted forward and backward substitutions ($\mathcal{H}$-FBS) are implemented to obtain the solution x of equation (3) with $O(kN\log N)$ computational complexity [26]. If the right-hand-side matrix B is replaced by a vector b, the process of solving (15) is the backward substitution, while the forward case is similar.

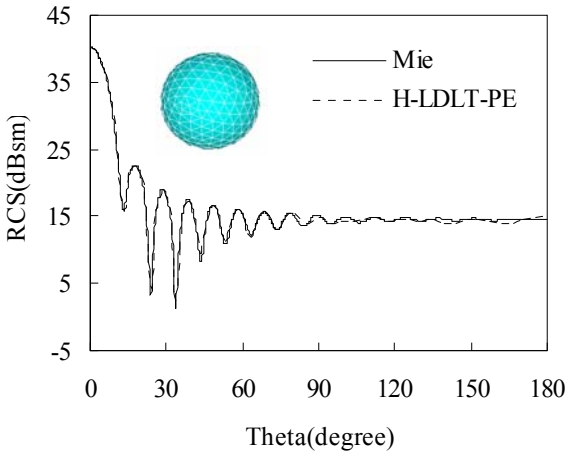

Fig. 3. Bistatic RCS of the sphere.

III. NUMERICAL RESULTS

In order to demonstrate the performances of the proposed method for 3D electrically large scattering problems, a variety of arbitrarily shaped objects are simulated. In these examples, scatters are all excited by the plane wave. The relative truncation error of ACA is set to be $\varepsilon_{\mathrm{ACA}}=10^{-3}$. The computations of the examples in this section are performed on a common PC with Intel Core2 2.8GHz CPU and 8GB RAM in double precision.

Table 1: Comparison of the computational costs for different methods

Method	Matrix construction		LDLT manipulation	
	Mem (MB)	Time (s)	Mem (MB)	Time (s)
MoM-LDLT	1.0×10^4	-	$>1.0\times10^4$	$>1.0\times10^5$
MoM-LDLT-PE	6.6	3.2	11.3	6.6
$\mathcal{H}$-LDLT	897.4	532.9	1054.6	1227.1
$\mathcal{H}$-LDLT-PE	4.4	9.6	4.9	3.9
Improvement Ratio	204.0	55.5	215.2	314.6

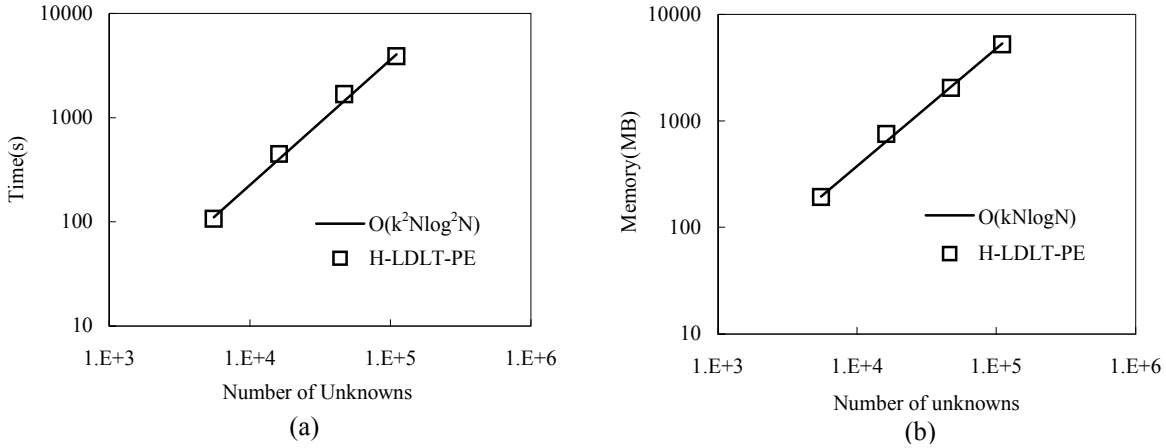

Fig. 4. The complexity tests of the $\mathcal{H}$-LDLT-PE with the number of unknowns increasing. (a) Time required for the $\mathcal{H}$-LDLT decomposition. (b) Memory required for $\mathcal{H}$-LDLT factors.

For simplification, the proposed method is referred to as the $\mathcal{H}$-LDLT-PE method.

The first example deals with the problem of scattering from a PEC sphere with a radius of $3m$. A plane wave is incoming in the direction $\theta=0^\circ$ and $\phi=0^\circ$ at a frequency of 300MHz. The conventional MoM solution may need 36,273 unknowns due to 0.1λ patch size. The proposed $\mathcal{H}$-LDLT-PE method needs only 927 unknowns since a patch size of about 0.6λ is achieved by using PE basis functions. The bistatic RCS is computed by the $\mathcal{H}$-LDLT-PE method and compared with the exact Mie series solution on the plane $\phi=0^\circ$. Very good agreement can be observed in Fig. 3. Direct solution of this example by conventional MoM on a common PC is an impossible mission, since a memory usage of about 10.0GB is required to store the impedance matrix and a rapid increase would occur in the direct solution. The bald ACA-based $\mathcal{H}$-LDLT method can reduce the total memory requirement for entire direct solution to about 2.0GB. By using the $\mathcal{H}$-LDLT-PE method, the computational costs can be further reduced dramatically. Table 1 shows the computational requirements of the MoM-based LDLT decomposition and presents the computational costs of the $\mathcal{H}$-LDLT method and the $\mathcal{H}$-LDLT-PE method for building an $\mathcal{H}$-matrix representation based on recompressed ACA and implementing the $\mathcal{H}$-LDLT decomposition under $\varepsilon_{\mathcal{H}}=10^{-3}$. The improvement ratio is also presented which validates the ability of the $\mathcal{H}$-LDLT method can be further improved by the $\mathcal{H}$-LDLT-PE method. Besides, we adopt the MLFMM combined with GMRES iteration to solve this problem. According to our test, 203.6MB memory usage and 19.2s CPU time usage are required for the construction of the

Table 2: Computational costs of the $\mathcal{H}$-LDLT-PE method for different $\varepsilon_{\mathcal{H}}$

$\mathcal{H}$-matrix construction		$\mathcal{H}$-LDLT manipulation		
Mem (MB)	Time (s)	$\varepsilon_{\mathcal{H}}$	Mem (MB)	Time (s)
520.4	624.6	5e-1	308.9	121.5
		1e-1	398.6	213.4
		1e-2	555.7	459.3
		1e-3	669.3	689. 5
		1e-4	785.2	877. 6

impedance matrix, and 582.39s CPU time is needed for the GMRES iterative solution with 10^{-3} residual norm.

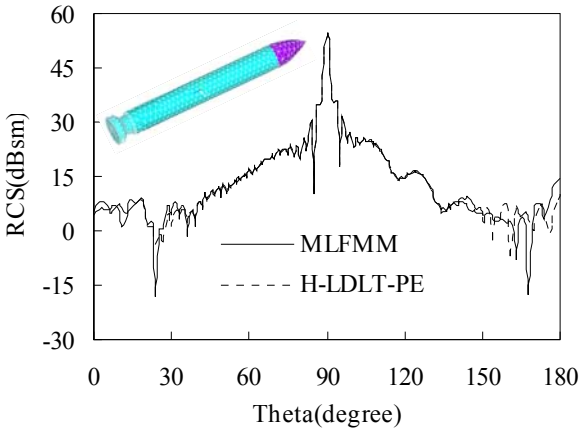

Fig. 5. Bistatic RCS of the missile.

It can be found that the $\mathcal{H}$-LDLT-PE has obvious advantages in the competition. Finally, the computational costs of the $\mathcal{H}$-LDLT-PE method are tested with the unknown number increasing from 5,531 to 110,362. As shown in Fig. 4 (a) and (b), the CPU time and memory usages are validated to be very close to $O(k^2 N \log^2 N)$ and $O(k N \log N)$, respectively.

The second example considers the scattering from a missile with a total length of $12.5m$ and a radius of $3m$ at the main body. The incident plane wave propagates from the direction $\theta = 90^\circ$ and $\phi = 0^\circ$ at 1 GHz. The conventional MoM solution needs 146,694 unknowns by using 0.1λ patch size, while the proposed $\mathcal{H}$-LDLT-PE method needs only 17,082 unknowns by using 0.6λ patch size at the smooth region of the missile. The bistatic RCS computed by the $\mathcal{H}$-LDLT-PE method on the plane $\phi = 0^\circ$ agrees very well with the results calculated by the MLFMM, as depicted in Fig. 5. Table 2 shows the computational costs for the construction of an $\mathcal{H}$-matrix and the $\mathcal{H}$-LDLT manipulation. The $\mathcal{H}$-LDLT-PE method not only provides an efficient solution of EFIE, but also can control the computational accuracy flexibly by different choices of the relative truncation error $\varepsilon_{\mathcal{H}}$ in the formatted $\mathcal{H}$-matrix arithmetic. Different $\varepsilon_{\mathcal{H}}$ requires different memory and CPU time usage, as shown in Table 2, and leads to different RCS error. Fig. 6 presents the RCS error integrated over all directions and normalized by the appointed accurate RCS calculated under $\varepsilon_{\mathcal{H}} = 10^{-8}$, without taking the truncation error of ACA into consideration. Since the parts of the top and bottom of this missile are not smooth, finer discretization can be employed for more accurate RCS, while the coarse discretization can be retained at the body of this missile without loss of accuracy. It is obvious that the direct solution of this 37λ problem based on MoM is drastically impossible, and the $\mathcal{H}$-LDLT method can hardly be performed on a common PC though the computational cost has been dramatically reduced. However, the $\mathcal{H}$-LDLT-PE method can be easily performed on a common PC at a very low cost as show in Table 2. For this example, the MLFMM requires 812.4MB memory and 192.6s CPU time to construct the impedance matrix, and 5410.6s CPU time to perform the GMRES iterations. Compared with the $\mathcal{H}$-LDLT-PE, although the MLFMM needs less construction time, it spends much more time for the iterative solution due to the slow convergence rate.

Finally, the scattering from a bent rectangular plate of $14m \times 7m$ is analyzed at 1 GHz. The plate

is bent leading to a dihedral conforming a wedge with an interior angle of 90°. The incident elevation angle is $\theta = 90^\circ$ and $\phi = 135^\circ$. A patch size of about 0.8λ is employed at the smooth region of the plate, which leads to only 27,189 unknowns. The bistatic RCS computed by the proposed $\mathcal{H}$-LDLT-PE method on the plane $\theta = 90^\circ$ is plotted together with the results of the MLFMM in Fig. 7. Table 3 shows the computational costs of the $\mathcal{H}$-LDLT-PE method under $\varepsilon_{\mathcal{H}} = 10^{-3}$. Obviously, the computational costs are extremely low by using the $\mathcal{H}$-LDLT-PE method, while the direct solution of this 42λ problem with 373,956 unknowns under the traditional 0.1λ patch size can hardly be accomplished on a common PC. For this problem, the MLFMM requires 1899.4MB memory and 366.9s CPU time to construct the impedance matrix, and 2796.8s

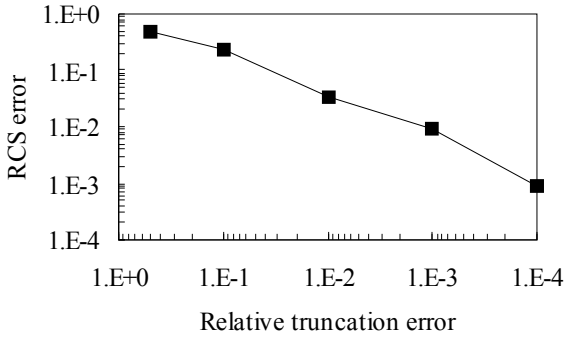

Fig. 6. Change of the RCS error with $\varepsilon_{\mathcal{H}}$ decreasing.

approximation technique with a recompression scheme is exploited to build the data-sparse representation of an $\mathcal{H}$-matrix, yielding a kernel-independent method. The $\mathcal{H}$-LDLT algorithm provides an inexpensive but sufficiently accurate way to compute and store the approximate triangular factor of the EFIE system matrix in nearly optimal complexity. The accuracy of the $\mathcal{H}$-LDLT is controllable by different choices of the relative truncation error, leading to different computational costs. PE basis function is employed to further reduce the memory and CPU time required for the $\mathcal{H}$-LDLT by introducing propagating wave phase dependence. Numerical results demonstrate the proposed method is robust for electrically large scattering problems.

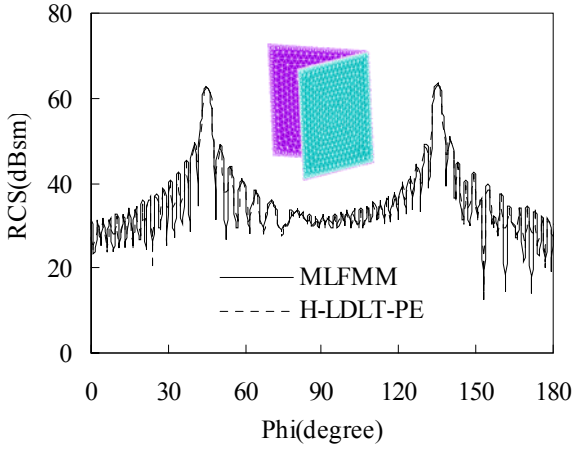

Fig. 7. Bistatic RCS of the bent rectangular plate.

Table 3: Computational costs of the $\mathcal{H}$-LDLT-PE method

$\mathcal{H}$-matrix construction		$\mathcal{H}$-LDLT manipulation	
Mem (MB)	Time (s)	Mem (MB)	Time (s)
631.1	842.5	855.7	860.2

$\varepsilon_{\mathcal{H}}$

CPU time to complete the GMRES iterative solution. It can be found that the $\mathcal{H}$-LDLT-PE defeats the MLFMM in overall computational costs, which demonstrate the capability of the H-LDLT-PE.

IV. CONCLUSION

A new direct method based on the $\mathcal{H}$-LDLT algorithm and PE basis functions is presented for the MoM solution of EFIE. The adaptive cross

ACKNOWLEDGMENT

We would like to thank the support of the Natural Science Foundation of 60871013, Jiangsu Natural Science Foundation of BK2008048.

REFERENCES

[1] S. M. Rao, D. R. Wilton, and A. W. Glisson, "Electromagnetic Scattering by Surfaces of Arbitrary Shape," *IEEE Trans. Antennas Propag.*, vol. 30, 409-418, 1982.

[2] S. M. Rao and R. F. Harrington, *Field Computation by Moment Methods*. New York: Macmillan, 1968.

[3] W. C. Chew, J. M. Jin, E. Midielssen, and J. M. Song, *Fast and Efficient Algorithms in Computational Electromagnetics*, Boston, MA: Artech House, 2001.

[4] J. M. Song, C. C. Lu, and W. C. Chew, "Multilevel Fast Multipole Algorithm for Electromagnetic Scattering by Large Complex Objects," *IEEE Trans. Antennas Propag.*, vol. 45, pp. 1488-1493, 1997.

[5] R. S. Chen, Z. H. Fan, Y. Y. An, M. M. Zhu, and K. W. Leung, "Modified Adaptive Cross Approximation Algorithm for Analysis of Electromagnetic Problems," *Applied Computational Electromagnetic Society (ACES) Journal*, vol. 26, no. 2, pp. 160-169, February 2011.

[6] H. Chen, Z. H. Fan, R. S. Chen, Z. N. Jiang, and M. M. Li, "Adaptive Mixed-Form Fast Multipole Method for the Analysis of Electromagnetic Scattering," *Applied Computational Electromagnetic Society (ACES) Journal*, vol. 25, no. 11, pp. 962-974, November 2010.

[7] Y. Saad, *Iterative Methods for Sparse Linear Systems*. New York: PWS Publishing, 1996.

[8] Michele Benzi, "Preconditioning Techniques for Large Linear Systems: A Survey", *Journal of Computational Physics*, 182, pp. 418-477, 2002.

[9] C. Delgado, E. García, F. Felipe Cátedra, and R. Mittra, "Application of the Characteristic Basis Function Method for the Electromagnetic Analysis of Electrically Large and Complex Bodies," *Applied Computational Electromagnetic Society (ACES) Journal*, vol. 24, no. 2, pp. 189-203, April 2009.

[10] K. R. Aberegg and A. F. Peterson, "Application of the Integral Equation-Asymptotic Phase Method to Two-Dimensional Scattering," *IEEE Trans. Antennas Propagat.*, vol. 43, pp. 534-537, 1995.

[11] J. M. Taboada, F. Obelleiro, J. L. Rodriguez, I. Garcia-Tunon, and L. Landesa, "Incorporation of Linear-Phase Progression in RWG Basis Functions," *Microwave and Optical Technology Letters*, vol. 44, no. 2, pp. 106-112, 2005.

[12] R. J. Burkholder, Ç. Tokgöz, C. J. Reddy, and W. O. Coburn, "Iterative Physical Optics for Radar Scattering Predictions," *Applied Computational Electromagnetic Society (ACES) Journal*, vol. 24, no. 2, pp. 241–258, April 2009.

[13] D. H. Kwon, R. J. Burkholder, and P. H. Pathak, "Efficient Method of Moments Formulation for Large PEC Scattering Problems using Asymptotic Phase Front Extraction (APE)," *IEEE Trans. Antennas Propag*, vol. 49, no. 4, pp. 583-591, 2001.

[14] Z. Nie, S. Yan, S. He, and J. Hu, "On the Basis Functions with Propagating Wave Phase Factor for Efficient Analysis of Scattering from Electrically Large Targets," *Progress In Elec-tromagnetics Research*, vol. 85, pp. 83-114, 2008.

[15] S. Yan, S. He, Z. Nie, and J. Hu, "Simulating Wide Band Radar Response from PEC Targets using Phase Extracted Basis Functions," *Progress In Electromagnetics Research*, vol.13, 409-431, 2009.

[16] W. Hackbusch, "A Sparse Matrix Arithmetic Based on $\mathcal{H}$-matrices. I. Introduction to $\mathcal{H}$-matrices," *Computing*, 62(2): pp. 89-108, 1999.

[17] S. Le Borne, "$\mathcal{H}$-Matrices for Convection-Diffusion Problems with Constant Convection," *Computing*, vol. 70, pp. 261-274, 2003.

[18] W. Chai and D. Jiao, "A $\mathcal{H}$-Matrix-Based Method for Reducing the Complexity of Integral-Equation-Based Solutions of Electromagnetic Problems," *IEEE International Symposium on Antennas and Propagation*, 2008.

[19] W. Hackbusch and B. Khoromskij, "A Sparse $\mathcal{H}$-Matrix Arithmetic. Part II: Application to Multi-Dimensional Problems," *Computing*, vol. 64, pp. 21-47, 2000.

[20] M. Bebendorf, "Approximation of Boundary Element Matrices," *Numer. Math.*, no. 86, pp. 565-589, 2000.

[21] M. Bebendorf and S. Rjasanow, "Adaptive Low-Rank Approximation of Collocation Matrices," *Computing*, vol. 70, no. 1, pp. 1-24, 2003.

[22] K. Z. Zhao, M. N. Vouvakis, and J. F. Lee, "The Adaptive Cross Approximation Algorithm for Accelerated Method of Moments," *IEEE Trans. Electromagn. Compat.*, vol. 47, no. 4, pp. 763-773, 2005.

[23] Z. N. Jiang, Z. H. Fan, D. Z. Ding, R. S. Chen, and K. W. Leung, "Preconditioned MDA-SVD-MLFMA for Analysis of Multi-Scale Problems," *Applied Computational Electromagnetic Society (ACES) Journal*, vol. 25, no. 11, pp. 914-925, November 2010.

[24] W. Hackbusch and Z. P. Nowak, "On the Fast Matrix Multiplication in the Boundary Element Method by Panel Clustering," *Numer. Math.*, vol. 54, pp. 463-491, 1989.

[25] S. Börm and W. Hackbusch, "$\mathcal{H}2$-Matrix Approximations of Integral Operators by Inter-Polation," Appl. Numer. Math., vol. 43, pp. 129-143, 2002.

[26] L. Grasedyck and W. Hackbusch, "Construction and Arithmetics of $\mathcal{H}$-Matrices," *Computing*, vol. 70, no. 4, pp. 295-344, 2003.

Ting Wan was born in Huanggang, Hubei, China. He received the B.S. and M.S. degrees in Electrical Engineering from Nanjing University of Science and Technology (NJUST), Nanjing, China, in 2003 and 2006, respectively. He is currently working toward the Ph.D. degree in the Department of Communication Engineering at NJUST. His research interests include computational electromagnetics, antennas, and microwave integrated circuits.

Rushan Chen was born in Jiangsu, China. He received his B.S. and M.S. degrees from the Dept. of Radio Engineering, Southeast University, in 1987 and in 1990, respectively, and his Ph.D. from the Dept. of Electronic Engineering, City University of Hong Kong in 2001. Since September 1996, he has been a Visiting Scholar with the Department of Electronic Engineering, City University of Hong Kong, first as Research Associate, then as a Senior Research Associate in July 1997, a Research Fellow in April 1998, and a Senior Research Fellow in 1999. From June to September 1999, he was also a Visiting Scholar at Montreal University, Canada. In September 1999, he was promoted to Full Professor and Associate Director of the Microwave & Communication Research Center in NJUST and in 2007, he was appointed Head of the Dept of Communication Engineering, Nanjing University of Science & Technology. His research interests mainly include microwave/millimeter-wave systems, measurements, antenna, RF-integrated circuits, and computational electro-magnetics. He is a Senior Member of the Chinese Institute of Electronics (CIE). He received the 1992 third-class science and technology advance prize given by the National Military Industry Department of China, the 1993 third class science and technology advance prize given by the National Education Committee of China, the 1996 second-class science and technology advance prize given by the National Education Committee of China, and the 1999 first-class science and technology advance prize given by JiangSu Province as well as the 2001 second-class science and technology advance prize. At NUST, he was awarded the Excellent Honor Prize for academic achievement in 1994, 1996, 1997, 1999, 2000, 2001, 2002, and 2003. He has authored or co-authored more than 200 papers, including over 140 papers in international journals. He is the recipient of the Foundation for China Distinguished Young Investigators presented by the National Science Foundation (NSF) of China in 2003. In 2008, he became a Chang-Jiang Professor under the Cheung Kong Scholar Program awarded by the Ministry of Education, China.

Xiaoqing Hu was born in Hubei, China, in June 1981. He received the B.S. and M.S. degrees in Applied Mathematics from Jilin University, Jilin, China, in 2004 and 2007, respectively. He is currently working toward the Ph.D. degree at Nanjing University of Science and Technology, Jiangsu, China. His research interests include integral equation and its fast methods.

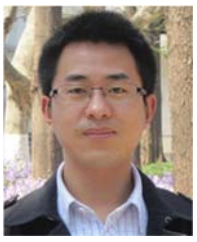

Yilin Chen was born in Jiangsu Province, the People's Republic of China. He is currently working toward the M.S. degree in the Department of Communication Engineering at Nanjing University of Science and Technology, Nanjing, China. His research interests include computational electromagnetics, antennas and microwave integrated circuits.

Yijun Sheng was born in Jiangsu Province, the People's Republic of China. He received the M.S. degree in Physics from Nanjing University of Science and Technology (NJUST) in 2003, and is currently working toward the Ph.D. degree in the Department of Communication Engineering at NJUST, Nanjing, China. His research interests include compu-tational electromagnetics, antennas, and microwave integrated circuits.